COLD MOLECULAR IONS: SINGLE MOLECULE STUDIES

M. DREWSEN

QUANTOP – Danish National Research Foundation for Quantum Optics, Department of Physics and Astronomy, University of Aarhus, Ny Munkegade, Build. 1520, DK-8000 Aarhus C, Denmark

Single molecular ions can be sympathetically cooled to a temperature in the mK-range and become spatially localized within a few μm^3 through the Coulomb interaction with laser-cooled atomic ions, and hence be an excellent starting point for a variety of single molecule studies. By applying a rather simple, non-destructive technique for the identification of the individual molecular ions relying on an *in situ* mass measurement of the molecules, studies of the photofragmentation of singly-charged aniline ions ($C_6H_7N^+$) as well as investigations of isotope effects in reactions of Mg^+ ions with HD molecules have been carried out.

Keywords: Single molecular ions; laser-cooling; photofragmentation; isotope effects.

1. Introduction

For the past decade, research involving cold molecules has gone through an extremely rapid developing phase. For neutral molecules the advances have, in particular, been relying on developments within the following approaches: Photo association of laser-cooled atoms,[1–5] buffer-gas cooling of molecules held in magnetic traps,[6–8] deceleration,[9] filtering[10] and trapping of molecules by electrostatic fields,[11–14] Feshbach resonance generated molecules in degenerated quantum gasses,[15,16] and deceleration of molecules by intense laser pulses.[17] Cooling techniques for molecular ions have been developed in parallel, so that e.g. it has become a standard to work with molecular ions which are sympathetically cooled into Coulomb crystals through the Coulomb interaction with laser-cooled atomic ions.[18–25] In the past years, the technique of He buffer gas ion cooling[26] has furthermore been extended to molecular anions.[27] Most recently, even the combination of cold neutral and ionic molecular techniques has made the first progress.[25]

After a presentation of our non-destructive single molecular ion mass

measurement technique,[20] the focus in this report will be on the latest results from our laboratory regarding experiments with single molecular ions.[23,24]

2. Non-destructive single-molecular ion-mass measurement

In order to experiment with single molecular ions, it has been necessary to develop a technique to identify the ion under investigation with high efficiency without destroying it. A schematic of such a non-destructive identification technique used in our single molecular ion experiments is presented in Figure 1. More detailed information on the technique can be found in.[20,28] The technique relies on the measurement of the resonant excitation frequency of one of the two axial oscillation modes of a trapped and crystallized linear two-ion system consisting of one laser-cooled atomic ion of known mass m1 and an *a priori* unknown molecular ion, whose mass m_2 has to be determined for ion identification. From this measured frequency, the mass m_2 of the unknown ion can be deduced from a simple relation between the frequency and the relative mass of the two ions:

$$\omega_{\pm}^2 = \left(1 + \frac{1}{\mu} + \sqrt{1 - \frac{1}{\mu} + \frac{1}{\mu^2}}\right)\omega_1^2, \tag{1}$$

where $\mu = m_2/m_1$, and ω_1 is the single ion oscillation frequency of the known ion. The solutions ω_+ and ω_- correspond to the mode with eigenvectors where the ions move in phase (COM mode) and out of phase (BR mode), respectively, with mass-dependent amplitudes.[29]

The crystallization of the two-ion system results from the sympathetic cooling of the molecular ion through the Coulomb interaction with the laser-cooled ion. This crystallization can be observed by imaging the fluorescence light emitted by the laser-cooled ion onto a CCD camera chip. Here, a well-localized spot appears with the atomic ion displaced a specific distance away from the trap center when it is trapped together with a non-fluorescing unknown ion. In the linear rf trap used in our experiments[19] the two-ion system is aligned along the traps main axis (the z-axis in Fig. 1). The resonant excitation can be promoted either by applying a sinusoidal electric field along this axis (through sinusoidal voltages applied to the end-electrodes of the trap), which will exert a force on both ions, or by periodically modulating the laser intensity of one of the cooling laser beams propagating along the main axis, which leads to a periodically varying scattering force on the laser-cooled ion. The resonance frequencies are determined by monitoring the fluorescence light from the laser-cooled ion

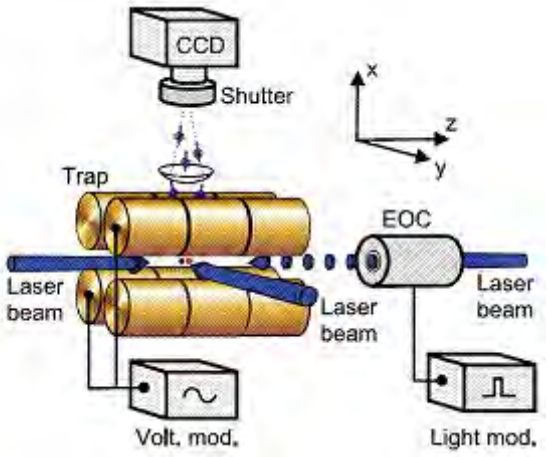

Fig. 1. Sketch of the experimental setup. Shown on the figure are the linear rf trap electrodes, the cooling laser beams and the CCD camera used to monitor the fluorescence from the laser-cooled atomic ions. An image-intensifier based shutter that can be gated phase-locked to a periodic driving force is installed in front of the camera. A driving force is applied either in the form of a sinusoidal voltage applied to the end-electrodes of the trap or through modulation of the scattering force on the atomic ion by using an electro-optic chopper (EOC) for scattering force modulation.

by the CCD camera while scanning the period of the applied driving force. When the period is equal to the period of one of the two oscillation modes (the center-of-mass (COM) mode and the breathing (BR) mode), the motion of the ions is most highly excited (neglecting damping exerted by the cooling lasers. Details on that see Refs. 20, 28. For CCD camera exposure times larger than the oscillation period of the ions, an enlarged axial extension of the fluorescence spot is observed close to these mode resonance frequencies as seen in Fig. 2. This detection method easily leads to a relative mass resolution $\Delta m/m$ below 10^{-2}, and can for optimized conditions even lead to a resolution at the 10^{-4} level.[28]

For long measuring times, more precise mass measurements are expected when the phase of the motion of the laser-cooled ion is monitored. This can be done by gating the CCD camera such that only light emitted at a certain phase with respect to the phase of the driving force is detected. Examples of such measurements can be seen in Fig. 3. Due to systematic errors, such measurements have so far also been limited to mass resolutions $\Delta m/m$ of a few times 10^{-4}.[20,28]

In the following sections, a few recent single molecular ion experiments,

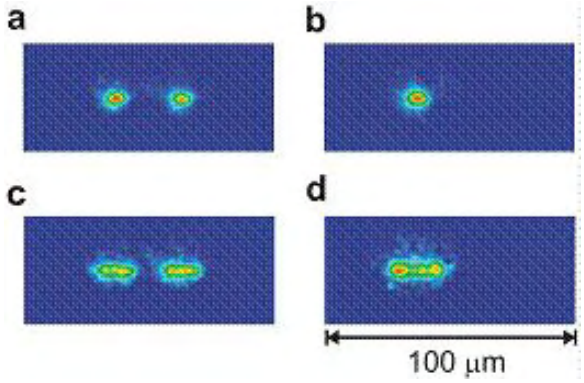

Fig. 2. (a) Fluorescence image of two laser-cooled Ca^+ ions. (b) An image of a laser-cooled Ca^+ ion trapped together with a sympathetically cooled *a priori* unknown singly charged ion. (c) and (d) are the images when the frequency of the electrical driving force is close to the COM mode frequency of the respective two-ion systems. For all images the camera integration time was 100 ms, which is much longer than the oscillation period of the ions of typical ∼10 ms.

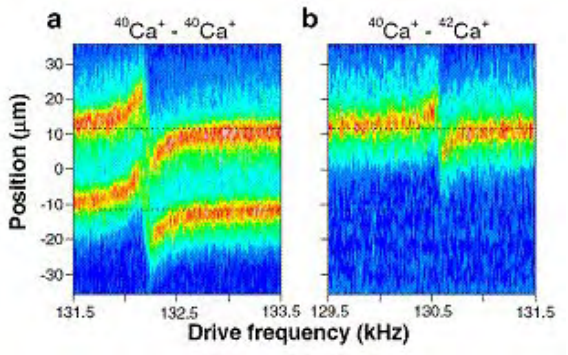

Fig. 3. The position resolved fluorescence along the trap axis (z axis) as a function of the drive frequency an intensity modulated cooling laser beam. (a) Two $^{40}Ca^+$ ions. (b) One $^{40}Ca^+$ ion and one $^{42}Ca^+$ ion, where only the $^{40}Ca^+$ ion is fluorescing. Each gray-scale (false-colored) contour plot is composed of axial projections of the fluorescence intensities in gated images recorded during the frequency scans. Dashed lines indicate equilibrium positions of the ions in the absence of modulation. The dark gray (red) areas near the dashed lines correspond to high intensity, while the dark (blue) areas are low intensity regions.

where the non-destructive mass measurement method is applied, will be discussed.

3. Consecutive photofragmentation of an aniline ion

The motivation for studying consecutive photofragmentation of aniline ions has been manifold. First, we wanted to prove that the non-destructive identification method described above allows detailed studies of the time evolution of light-induced consecutive fragmentation at long time scales (milliseconds up to several hours). Secondly, we wanted to prove that non-destructive detection of photofragments is a viable way for probabilistic preparation of a wealth of single-molecular ions which can be used as targets for other experiments (e.g., astrophysical studies). Thirdly, more generally, we wanted to prove that studies of spatially localized and very cold single ions can be extended from diatomic systems[20] to complex molecular systems. In all, this opens up new opportunities in molecular science, including molecular rotational dynamics and chemical reaction dynamics on long time scales.

In the experiments, a single aniline ion ($C_6H_5NH_2^+$) is irradiated by the combination of cw light at 397 nm (originating from the laser beams used to cool the calcium ions which provide the sympathetic cooling), and nanosecond pulses of light at 294 nm (used to produce the aniline ions in the first place through a 1+1 REMPI process).[23] In Fig. 4(a), the frequency, at which a specific molecular ion mass has been detected during a series of 77 experiments, is presented. As clearly seen, a series of molecular ions, and not only $C_6H_5NH_2^+$ ions (mass 93 amu), are produced. By repeatable mass scans we can follow the photofragmentation of the original aniline ion in time as the few examples in Fig. 4(b) show. In Fig. 5, a simplified picture is presented of how the photofragmentation is progressing. In a single experiment we were indeed able to monitor all the indicated molecular ions, but the initially produced aniline ion, as seen in Fig. 6.[23] While $C_6H_5NH_2^+$, $C_5H_6^+$, and $C_5H_5^+$ ions were only sometimes found to be stable against further photofragmentation (corresponding to a probabilistic preparation of those ions), the $C_3H_3^+$ ion was always stable.

How sequential breakage of larger molecules into lighter fragments takes place can potentially be monitored non-destructively on time scales ranging from less than a second to several hours by the applied technique.

4. Isotope effects in reaction of Mg^+ ions with HD molecules

Studies of isotope effects in chemical reactions can often help to obtain a better understanding of the underlying reaction dynamics. Resonance

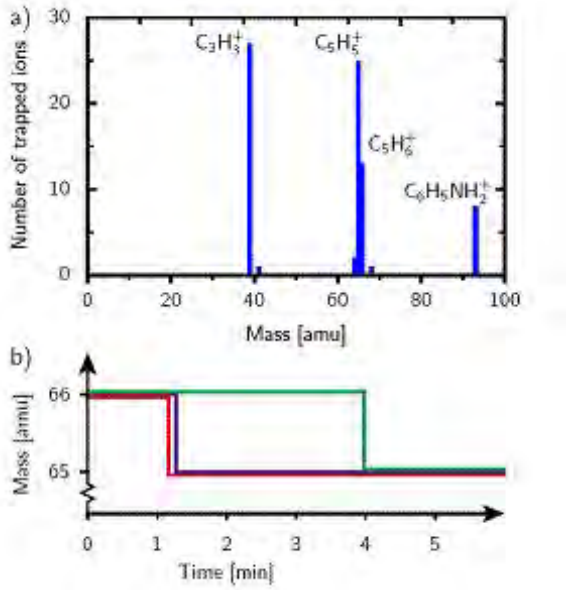

Fig. 4. (a) Molecular ion mass spectrum with aniline ions ($C_6H_5NH_2^+$ ions) produced through a 1+1 REMPI process as the starting point. The height of the bars indicates how often a specific ion mass was detected in a series of experiments. (b) Three recorded time sequences of the photodissociation of $C_5H_6^+$. The statistical nature of the dissociation process is clearly visible by the three single molecule experiments.

effects observed in the F + H_2 reaction and isotopic analogs have e.g. resulted in a much improved understanding of this benchmark reaction.[30–32] In a series of experiments, we have studied reactions between Mg^+ in the $3p^2P_{3/2}$ excited state (excitation energy of 4.4 eV) with isotopologues of molecular hydrogen at thermal energies. Due to the simple internal structure of the reaction partners, these reactions represent a particularly simple test case for reaction dynamics involving an electronically excited atomic collision partner, and hence can serve as good benchmark reactions for reaction dynamics simulations. In brief, we here consider only reactions of the types represented by the Eqs. (2) and (3). Reactions with other isotopologues of molecular hydrogen can be found in Ref. 24. From the results presented in Fig. 7, corresponding to a total of only about 300 single ion reactions, the branching ratio between the reactions

$$Mg^+\left(3p^2P_{3/2}\right) + HD \rightarrow MgD^+ + H \tag{2}$$

$$Mg^+\left(3p^2P_{3/2}\right) + HD \rightarrow MgH^+ + D \tag{3}$$

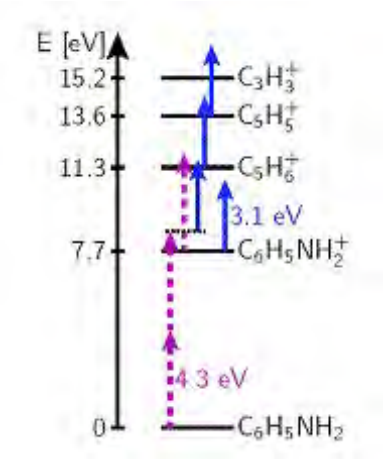

Fig. 5. Energy level scheme with indication of the ground state energies of several relevant molecular ions relative to the ground state of neutral aniline. The dashed (solid) arrows indicate some of the photodissociation paths observed in the experiments due to the presence of light at 294 nm (397 nm).

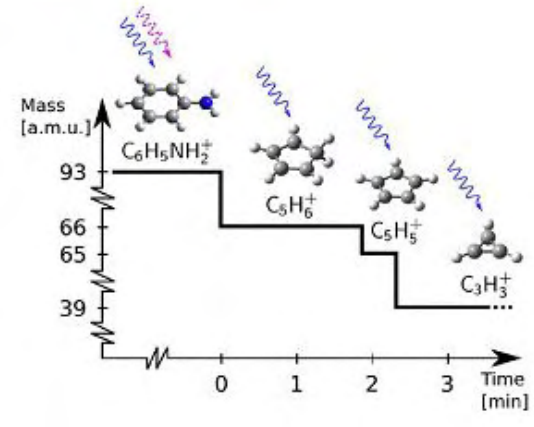

Fig. 6. A consecutive photodissociation sequence observed in an experiment. The dashed (solid) wriggly arrows represent 294 nm (397 nm) photons responsible for the fragmentations.

has been found to be larger than 5. This strong isotope effect cannot be explained by a simple statistical model based on an assumption of an equal probability for populating energetically accessible states of MgH^+

and MgD^+, but must be attributed to a dynamical mechanism. In the ion beam experiments of Ref. 33 a similar isotope effect was observed in reactions between ground state Mg^+ ions and HD molecules at center-of-mass energies up to 11 eV. This was rationalized in terms of an impulsive interaction with a thermodynamic threshold.

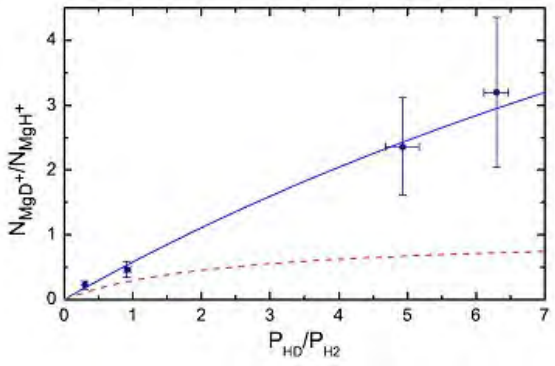

Fig. 7. The ratio between the number of formed $^{26}MgD^+$ and $^{26}MgH^+$ ions as a function of the relative pressure of HD and H_2. From left to right, the data points correspond to the following numbers of times measuring MgD^+ / MgH^+: 17/75, 21/45, 33/14 and 32/10. The error bars represent statistical uncertainties. The blue (solid) and the red (dashed) curves represent results from a simple theoretical model based on Langevin capture (See Eq. (3) in Ref. 24). While the dashed curve is the expected result for equal probability of forming $^{26}MgD^+$ and $^{26}MgH^+$ after Langevin capture of HD, the solid curve shows the best fit to the experimental data. The error bars of the measurements taken into account, the fit suggests a ratio of the formation rate of $^{26}MgD^+$ and $^{26}MgH^+$ ions in the range of ~ 6 to ∞ for the $Mg^+(3p^2P_{3/2})$ + HD reaction.

A schematic view of the potential surfaces involved in the reaction is shown in Fig. 8. Investigations of photofragmentation of MgD_2^+ indicate that the Mg^+ + HD reaction discussed here proceeds via the 1^2B_2 surface through a bond-stretch mechanism that eventually favors the formation of MgD^+.[34,35] To fully understand the transition from an $MgHD^+$ complex to a potential surface favoring the MgD^+ + H asymptote rather than the MgH^+ + D asymptote, a detailed theoretical study is required. It might be necessary to consider the details of the conical intersection which arises from the crossing of the 1^2A_1 and 1^2B_2 potential surfaces. Non-adiabatic couplings at the conical intersection could give rise to a preference of the MgD^+ channel over the MgH^+ channel. The same mechanism could as well be responsible for the isotope effect observed in reactions with ground state

Mg^+ ions.[33]

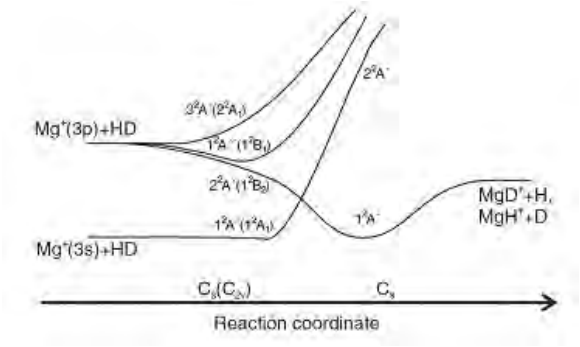

Fig. 8. Sketch of relevant potential surfaces in C_s symmetry for the $Mg^+ + HD$ reaction proceeding by insertion of Mg^+ into the HD bond on the $2\,^2A'$ potential surface, followed by Mg^+-D or Mg^+-H bond formation. On the left-hand side the C_{2v} symmetry labels in parentheses are valid for the analogous reaction with H_2 or D_2.[35]

The above discussed reaction experiments demonstrate the prospects for similar single molecular ion studies using state prepared molecular ions,[36,37] complex molecular ions[22,23] or molecules of astrophysical interest.[38,39] The high detection efficiency can furthermore be useful for studies of reactions involving ions of rare species, e.g. super-heavy elements.[40]

Acknowledgements

The presented work has been support by the Danish National Research Foundation trough QUANTOP, the Danish Natural Science Research Council, and the European Science Foundation.

References

1. T. Takekoshi, B. M. Patterson and R. J. Knize, *Phys. Rev. Lett.* **81**, 5105 (1998).
2. A. Fioretti, D. Comparat, A. Crubellier, O. Dulieu, F. Masnou-Seeuws and P. Pillet, *Phys. Rev. Lett.* **80**, 4402 (1998).
3. A. N. Nikilov, E. E. Eyler, X. T. Wang, J. Li, H. Wang, W. C. Stwalley and P. L. Gould, *Phys. Rev. Lett.* **82**, 703 (1999).
4. M. J. Wright, J. A. Pechkis, J. L. Carini, S. Kallush, R. Kosloff and P. L. Gould, *Phys. Rev. A* **75**, 051401 (2007)
5. M. Viteau, A. Chotia, M. Allegrini, N. Bouloufa, O. Dulieu, D. Comparat and P. Pillet, *Science* **321**, 232 (2008).

6. J. D. Weinstein, R. deCarvalho, T. Guillet, B. Friedrich and J. M. Doyle, *Nature* **395**, 148 (1998).
7. D. Egorov, J. D. Weinstein1, D. Patterson1, B. Friedrich1 and J. M. Doyle, *Phys. Rev. A* **63**, 030501(R) (2001).
8. W. C. Campbell, G. C. Groenenboom, H.-I. Lu, E. Tsikata and J. M. Doyle, *Phys. Rev. Lett.* **100**, 083003 (2008).
9. H. L. Bethlem, G. Berden and G. Meijer, *Phys. Rev. Lett.* **83**, 1558 (1999).
10. S. A. Rangwala, T. Junglen, T. Rieger, P. W. Pinkse and G. Rempe, *Phys. Rev. A* **67**, 043406 (2003).
11. H. L. Bethlem, G. Berden, F. M. H. Crompvoets, R. T. Jongma, A. J. A. van Roij and G. Meijer, *Nature* **406**, 491 (2000).
12. F. M. H. Crompvoets, H. L. Bethlem, R. T. Jongma and G. Meijer, *Nature* **411**, 174 (2001).
13. T. Rieger, T. Junglen, S. A. Rangwala, P. W. Pinkse and G. Rempe, *Phys. Rev. Lett.* **95**, 173002 (2005).
14. S. Hoekstra, J. J. Gilijamse, B. Sartakov, N. Vanhaecke, L. Scharfenberg, S. Y. van de Meerakker and G. Meijer, *Phys. Rev. Lett.* **98**, 133001 (2007).
15. M. Greiner, C. A. Regal and D. S. Jin, *Nature* **426**, 537 (2003).
16. S. Jochim, M. Bartenstein, A. Altmeyer, G. Hendl, S. Riedl, C. Chin, J. H. Denschlag and R. Grimm, *Science* **302**, 2101 (2003).
17. R. Fulton, A. I. Bishop and P. F. Barker, *Phys. Rev. Lett.* **93**, 243004 (2004).
18. K. Mlhave and M. Drewsen, *Phys. Rev. A* **62**, 011401(R) (2000).
19. M. Drewsen, I. Jensen, J. Lindballe, N. Nissen, R. Martinussen, A. Mortensen, P. Staanum and D. Voigt, *Int. J. Mass. Spect.* **229**, 83 (2003).
20. M. Drewsen, A. Mortensen, R. Martinussen, P. Staanum and J. L. Srensen, *Phys. Rev. Lett.* **93**, 243201 (2004).
21. P. Blythe, B. Roth, U. Frhlich, H. Wenz and S. Schiller, *Phys. Rev. Lett.* **95**, 183002 (2005).
22. A. Ostendorf, C. B. Zhang, M. A. Wilson, D. Offenberg, B. Roth and S. Schiller, *Phys. Rev. Lett.* **97**, 243005 (2006).
23. K. Hjbjerre, D. Offenberg, C. Z. Bisgaard, H. Stapelfeldt, P. F. Staanum, A. Mortensen and M. Drewsen, *Phys. Rev. A* **77**, 030702(R) (2008).
24. P. F. Staanum, K. Hjbjerre, R. Wester and M. Drewsen, *Phys. Rev. Lett.* **100**, 243003 (2008).
25. S. Willitsch, M. T. Bell, A. D. Gingell, S. R. Procter and T. P. Softley, *Phys. Rev. Lett.* **100**, 043203 (2008).
26. See, for example, D. Gerlich, *Phys. Scr.* **59**, 256 (1995), and references therein.
27. S. Trippel, J. Mikosch, R. Berhane, R. Otto, M. Weidemller and R. Wester, *Phys. Rev. Lett.* **97**, 193003 (2006).
28. P. F. Staanum, K. Hjbjerre and M. Drewsen, to appear in *Practical Aspects of Trapped ion Mass Spectrometry IV*, ed. R. March and J. Todd (Taylor & Francis, 2008).
29. D. Kielpinski, B. E. King, C. J. Myatt, C. A. Sackett, Q. A. Turchette, W. M. Itano, C. Monroe, D. J. Wineland and W. H. Zurek, *Phys. Rev. A* **61**, 032310 (2000).

30. W. Hu and G. C. Schatz, *J. Chem. Phys* **125**, 132301 (2006), and references therein.
31. D. M. Neumark, A. M. Wodtke, G. N. Robinson, C. C. Hayden and Y. T. Lee, *Phys. Rev. Lett.* **53**, 226 (1984).
32. M. Qui, Z. Ren, L. Che, D. Dai, S. Harich, X. Wang, X. Yang, C. Xu, D. Xie, M. Gustafsson, R. T. Skodje, Z. Sun and D. H. Zhang, *Science* **311**, 1440 (2006).
33. N. Dalleska, K. Crellin and P. Armentrout, *J. Phys. Chem.* **97**, 3123 (1993).
34. L. N. Ding, M. A. Young, P. D. Kleiber and W. C. Stwalley, *J. Phys. Chem.* **97**, 2181 (1993).
35. P. D. Kleiber and J. Chen, *Int. Rev. Phys. Chem.* **17**, 1 (1998).
36. I. S. Vogelius, L. B. Madsen and M. Drewsen, *Phys. Rev. Lett.* **89**, 173003 (2002).
37. I. S. Vogelius, L. B. Madsen and M. Drewsen, *Phys. Rev. A* **70**, 053412 (2004).
38. D. Gerlich, E. Herbst and E. Roueff, *Planet. Space Sci.* **50**, 1275 (2002).
39. S. Trippel *et al.*, *Phys. Rev. Lett.* **97**, 193003 (2006).
40. M. Drewsen, *Eur. Phys. J. D* **45**, 125 (2007).